

# Occurrence of a chiral-like pair band and a six-nucleon noncollective oblate isomer in $^{120}\text{I}$

B. Moon<sup>a</sup>, C.-B. Moon<sup>b,\*</sup>, G.D. Dracoulis<sup>c</sup>, R.A. Bark<sup>c,d</sup>, A.P. Byrne<sup>c</sup>, P.A. Davidson<sup>c</sup>, G.J. Lane<sup>c</sup>, T. Kibédi<sup>c</sup>, A.N. Wilson<sup>c</sup>, C. Yuan<sup>e</sup>, B. Hong<sup>a</sup>

<sup>a</sup> Department of Physics, Korea University, Seoul 02841, Republic of Korea

<sup>b</sup> Faculty of Science, Hoseo University, Chung-Nam 31499, Republic of Korea

<sup>c</sup> Department of Nuclear Physics, Research School of Physical Sciences and Engineering, The Australian National University, Canberra, ACT 2601, Australia

<sup>d</sup> iThemba LABS PO Box 722, Somerset West 7129, South Africa

<sup>e</sup> Sino-French Institute of Nuclear Engineering and Technology, Sun Yat-sen University, Zhuhai 519-082, China

## ARTICLE INFO

### Article history:

Received 4 April 2018

Received in revised form 5 June 2018

Accepted 7 June 2018

Available online 14 June 2018

Editor: V. Metag

### Keywords:

Iodine

Isomer

Chiral-like pair band

In-beam  $\gamma$ -ray spectroscopy

## ABSTRACT

We report for the first time two distinctive features in the odd–odd nucleus  $^{120}\text{I}$ : a pair of doublet bands and a high-spin isomer built on the  $\pi h_{11/2} \nu h_{11/2}$  configuration. For producing the excited states of  $^{120}\text{I}$ , a fusion-evaporation reaction  $^{118}\text{Sn}(^6\text{Li}, 4n)$  at  $E_{\text{lab}} = 48$  MeV was employed. The beam was provided by the 14UD tandem accelerator of the Heavy Ion Accelerator Facility at the Australian National University. The observed doublet structure built on the positive-parity states is the first case and unique in isotopes with  $Z = 53$ . The emerging properties are indicative of the known chiral characteristics, leading to a doubling of states for the  $\pi h_{11/2} \nu h_{11/2}$  configuration. In contrast, the high-spin isomer with a half-life of 49(2) ns at spin-parity  $J^\pi = 25^+$  can be explained in terms of a noncollective oblate structure with the full alignment of six valence nucleons outside the  $^{114}\text{Sn}$  core: three protons  $(g_{7/2})^1(d_{5/2})^1(h_{11/2})^1$  and three neutrons  $(h_{11/2})^3$ . This is an outstanding case that reveals a pure single-particle structure consisting of equal numbers of valence protons and neutrons outside the semi-double shell closure of  $^{114}\text{Sn}$  with  $Z = 50$  and  $N = 64$ .

© 2018 The Author(s). Published by Elsevier B.V. This is an open access article under the CC BY license (<http://creativecommons.org/licenses/by/4.0/>). Funded by SCOAP<sup>3</sup>.

Nuclei close to the  $Z = 50$  shell closure are good candidates for investigations of nuclear shell structure because isomeric states induced by a few particles (or holes) outside a closed core are abundant. The long-lived nature of isomers has been interpreted as arising from the shape coexistence, spin-trap, and  $K$ -trap isomerism [1–3]. Spin (or yrast) trap isomers are normally found near closed shells, e.g., in Sn, Sb, and I around  $Z = 50$ . The unique negative-parity neutron  $h_{11/2}$  orbital, which lies close to the Fermi surface, is responsible for the spin-trap isomerism in this region. These unusual high-spin states are interpreted as being associated with the noncollective oblate state owing to an oblate mass distribution that is symmetric around the rotation axis.

Moreover, the neutron-deficient odd–odd I isotopes fall in a region where the  $h_{11/2}$  proton ( $\pi h_{11/2}$ ) and the  $h_{11/2}$  neutron ( $\nu h_{11/2}$ ) orbitals near the Fermi surface are of opposite particle–hole character. This condition can lead to complicated dynamics and is the basis for the development of the so-called chiral bands

in the mass  $A = 120 - 130$  region. As described by Frauendorf and collaborators [4–6], the chiral mechanism comes from a combination of dynamics: the angular momentum involving two quasi-particles in the appropriate orbitals and geometry (i.e. the triaxial shape). Under this condition, high- $j$  particles of one kind of nucleon and high- $j$  holes of the other kind are combined with the triaxial deformed potential in odd–odd nuclei. One of experimental signatures of the chirality is the observation of a pair of  $\Delta I = 1$  collective bands with the same parity and a small energy difference. To date, chiral-like doublet bands have been systematically observed in the mass  $A \sim 130$  region such as in Cs, La, Pr, and Pm [7–11].

In the present work, we report on observation of both a specific single-nucleon configurational state and a collective state in odd–odd  $^{120}\text{I}$ : a noncollective oblate isomer at a high-spin state and a pair of doublet bands, which are both unique in the  $Z = 53$  odd–odd system. It should be emphasised that the first observation of the doublet bands in  $^{120}\text{I}$  was given in our previous report [12].

The experiment was conducted at the Heavy Ion Accelerator Facility of the Australian National University. The excited states of

\* Corresponding author.

E-mail address: cbmoon@hoseo.edu (C.-B. Moon).

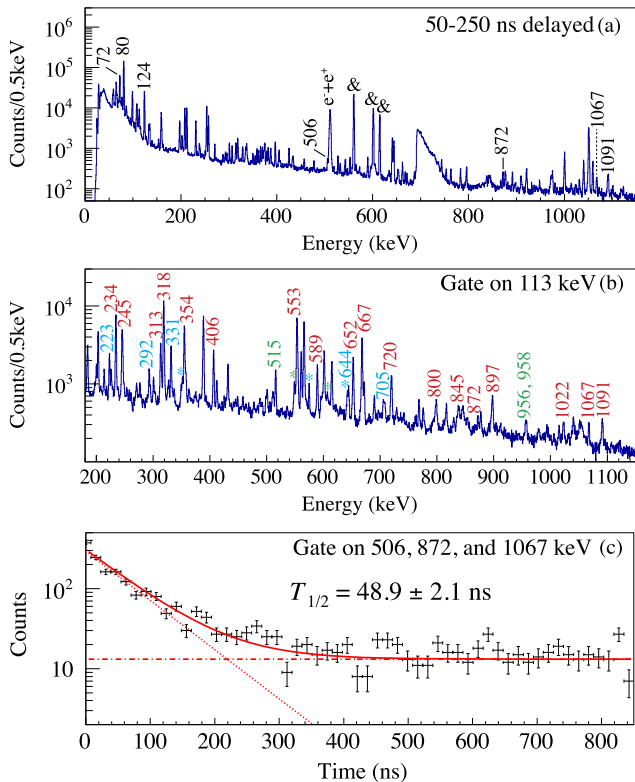


**Fig. 1.** (Colour online) (a) Delayed singles  $\gamma$ -ray spectrum of  $^{120}\text{I}$ . The  $\gamma$  transitions from isomers are indicated. The internal transitions from  $^{120}\text{Te}$  are marked with & symbols. (b) Coincidence  $\gamma$ -ray spectrum with the gate condition of 113 keV. Transitions from Band 1 (2) are indicated with red (blue) numbers or asterisk marks. Green numbers or asterisk marks represent the inter-transitions between Band 1 and Band 2. (c) Decay curve with gate conditions of 506, 872, and 1067 keV.

$^{120}\text{I}$  were populated by the  $^{118}\text{Sn}(^6\text{Li}, 4n)$  reaction at a beam energy of 48 MeV. The beam, provided by the 14UD tandem accelerator, had a pulsed structure with a 1-ns pulse separated by periods of 1.7  $\mu\text{s}$ . The  $^{118}\text{Sn}$  target was a self-supporting foil with a thickness of 3.6 mg/cm $^2$ .  $\gamma$  rays emitted during the decay of excited states were detected by using the CAESAR array, which was composed of six Compton-suppressed hyper-purity germanium (HPGe) detectors and two low-energy photon spectrometer (LEPS) detectors.  $\gamma$  rays were collected both during the period that the beam was incident on the target and during the period without beam irradiation, allowing the detection of decays following isomeric states.

Fig. 1(a) shows the  $\gamma$ -ray singles spectrum of  $^{120}\text{I}$  within the delayed region in timing information. Retarded  $\gamma$  transitions induced by several isomeric states in  $^{120}\text{I}$  are obtained and their energies are indicated. The peaks marked with & symbols are  $\gamma$  rays emitted from  $^{120}\text{Te}$ , which is another resultant nucleus from the reaction or a daughter nucleus after the  $\beta$  decay. The 72-keV isomeric decay with a half-life of 244(3) ns has been previously reported in [13,14]. This isomer is located at 72 keV and has a spin-parity of  $3^+$ . The 80- and 124-keV transitions are delayed  $\gamma$  rays from the  $7^-$  isomeric state at 290 keV with a half-life of 9.2 ns [13,14]. The 506-, 872-, 1067-, and 1091-keV peaks are from the high-spin isomer located at the top of the collective band with positive parity.

$\gamma$  rays belonging to Band 1 and Band 2 can be found in Fig. 1(b) by gating on the 113-keV transition, de-exciting the  $9^+$  state, which is populated by both bands as shown in Fig. 2. Here, Band 1 and Band 2 are collective bands of interest built on the  $\pi h_{11/2} \nu h_{11/2}$  configuration. Based on the mean of the  $\gamma$ - $\gamma$  coinci-

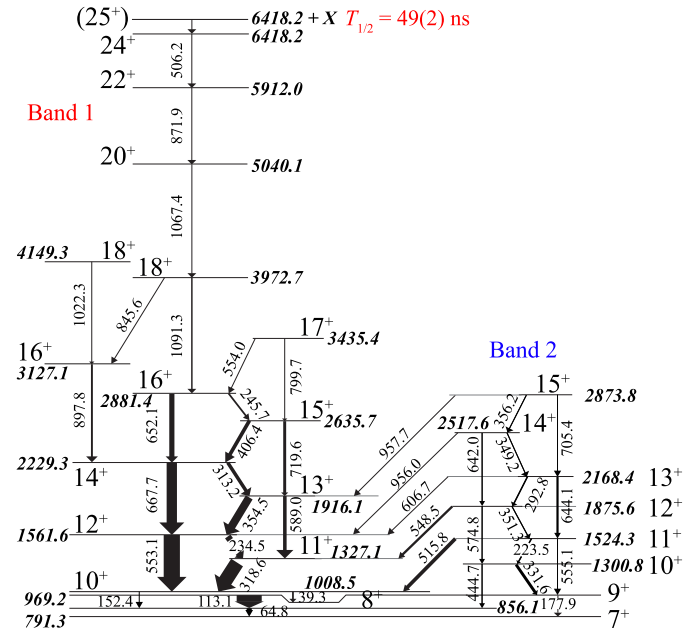


**Fig. 2.** (Colour online) Partial level scheme of  $^{120}\text{I}$  indicating only excited states built on the  $\pi h_{11/2} \nu h_{11/2}$  configuration. Full level schemes are found in [13] and in our supplementary materials. All the energy scales are in keV.

dence analysis,  $\gamma$  transitions not only from Band 1 and Band 2 but also from weak inter-transitions between these two bands were successfully identified. The detailed full level scheme and the characteristics of  $\gamma$ -ray transitions can be found in the *supplementary materials*. It should be noticed that the present level scheme of  $^{120}\text{I}$  differs from the result reported by Kaur et al. [15]. In Ref. [15], the dominant states, to which we assign positive parity, were assigned to be of negative parity with a band head of  $9^-$  and interpreted as being associated with the  $\pi g_{7/2} \nu h_{11/2}$  configuration. However, we suggested [12,13] that Band 1 should be associated with the  $\pi h_{11/2} \nu h_{11/2}$  configuration for the following reasons: Firstly, the multipolarities of  $\gamma$  transitions were determined by the DCO (directional correlation of oriented states) analysis. For instance, in the full level scheme [13], two strong transitions with 565.5 and 571.1 keV, depopulating the  $8^+$  and  $9^+$  states, show  $E1$  dipole character. Secondly, the level built on the  $11/2^-$  state dominates the yrast sequence in adjacent odd-proton ( $^{119,121}\text{I}$  [16,17]), and odd-neutron ( $^{119}\text{Te}$  [18] and  $^{121}\text{Xe}$  [19]) nuclides. Further, the excitation energy of the  $10^+$  band-head state is systematically consistent with that of the negative-parity band-head state based on the  $h_{11/2}$  orbital in the neighbouring odd-mass  $^{119,121}\text{I}$  isotopes. Finally, to understand the origin of  $9^+$  and  $10^+$ , we performed theoretical calculations with a large-scale spherical shell model (SM) in the space of  $50 < Z$  and  $N < 82$  using the shell model code, K-SHELL [20]. It was found that the calculated  $9^+$  and  $10^+$  states, dominated by the  $\pi h_{11/2} \nu h_{11/2}$  configuration, comprising 49% and 60%, respectively, have been built at 1004 and 1003 keV. These levels are almost consistent with the observed  $9^+$  and  $10^+$  states.

Above Band 1, a high-spin isomer was found at 6418 keV. This observation was from an analysis of the time-correlated  $\gamma$ -ray spectrum data in which the 506- and 872-keV transitions appear to be delayed characters, as shown in Fig. 1(a). Fig. 1(c) shows the decay curve induced by the retarded transitions depopulating the observed isomer. The half-life of this isomer is estimated to be 49(2) ns by using the maximum likelihood method with an exponential decay function and a constant background. Li et al. [21] suggested that, by noticing the imbalanced intensities between transitions populating and depopulating the 6418-keV level,

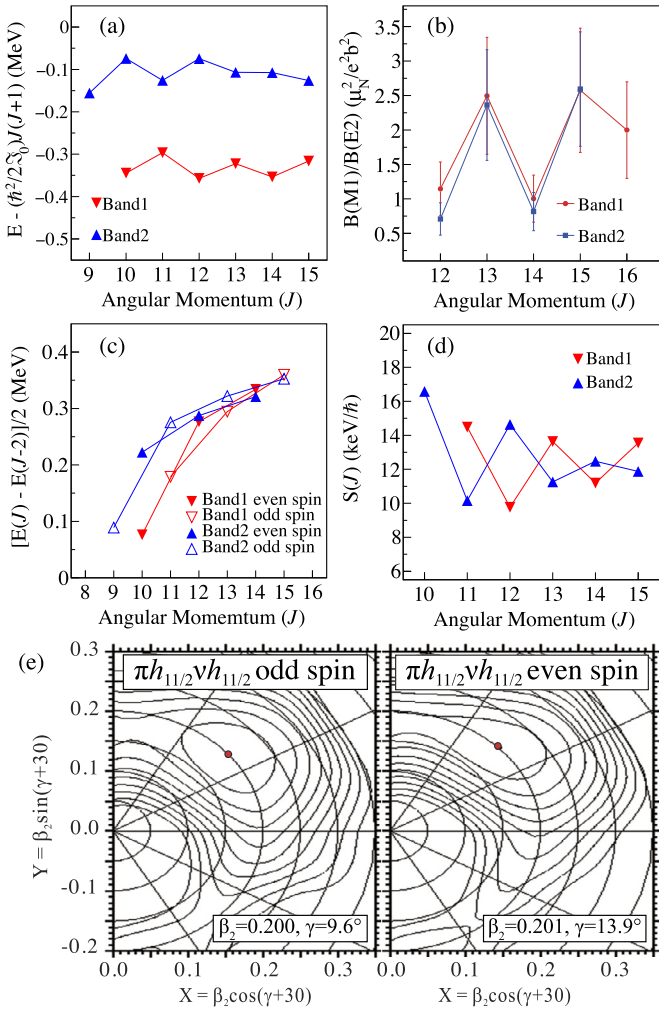


**Fig. 3.** (Colour online) (a) Plot of excitation energies relative to liquid-drop model energies as a function of  $J$  with  $\hbar^2/2\mathcal{J}_0 \approx 12$  keV. Here,  $\mathcal{J}_0$  is the moment of inertia. (b)  $B(M1)/B(E2)$  values for the  $\pi h_{11/2}\nu h_{11/2}$  band and its doublet band in  $^{120}\text{I}$ . (c) Plot of  $\hbar\omega = [E(J) - E(J-2)]/2$  that shows the angular frequencies. (d) Plot of the staggering parameters,  $S(J) = [E(J) - E(J-1)]/2J$ . (e) Plots of the calculated total energy surface for the  $\pi h_{11/2}\nu h_{11/2}$  configuration in  $^{120}\text{I}$  at  $\hbar\omega = 0.24$  MeV. The left panel is for favoured states with odd spins and the right panel is for unfavoured states with even spins.

this 6418-keV level would be an isomeric state. Accordingly, the 506-keV transition was proposed to be an  $M3$  transition. However, based on our further discussion, the 506-keV transition should have an  $E2$  character and the isomer would be depopulated by an unobserved low-energy  $M1$  transition. Given the low-energy detection efficiency of the LEPS, this low  $M1$  transition may be below 30 keV. Consequently, this isomer is considered to be  $J^\pi = 25^+$  at an energy of  $\Delta E < 30$  keV above the 6418-keV state.

Fig. 3 shows the main characteristics of Band 1 and Band 2: (a)  $E(J) - (\hbar^2/2\mathcal{J}_0)J(J+1)$ , (b) the  $B(M1)_{in}/B(E2)_{in}$  ratios, (c) the angular frequencies,  $\hbar\omega = [E(J) - E(J-2)]/2$ , (d) the staggering parameters,  $S(J) = [E(J) - E(J-1)]/2J$ , and (e) the total Routhian energy surface (TRS) calculations [22]. Based on the results shown in Figs. 3(a)–(d), we can conclude that Band 2 is a candidate for a chiral-like pair band of Band 1. In Fig. 3(a), the energy separation between two bands and the signature splitting can be found. Band 2 is found to be lying higher in energy by  $\sim 250$  keV than the main  $\pi h_{11/2}\nu h_{11/2}$  band, Band 1. This energy separation is similar to values between the chiral doublet bands in odd-odd Cs, La, Pr, and Pm nuclei [7–11]. The observed similarity in the energy

separation between Band 1 and Band 2 reflects their common underlying structure in the mass  $A \sim 130$  nuclei; therefore, Band 2 may be associated with the chiral partner band leading to a doubling of states for the  $\pi h_{11/2}\nu h_{11/2}$  configuration. Our suggestion can be further supported by discussing the  $B(M1)_{in}/B(E2)_{in}$  ratio. The  $B(M1)_{in}/B(E2)_{in}$  values for Band 1 and Band 2 are almost same as shown in Fig. 3(b). Various types of reduced transition ratios are summarised in Table 1. Fig. 3(c) shows the change of collective angular momentum geometries in two bands. For example, two lowest points in each band show their planar geometries at the band heads. However, as the spin increases, each band dramatically changes the angular momentum geometry into an aplanar geometry which causes the chiral doubling. The staggering parameter,  $S(J)$ , is also one of fingerprints for the chiral doubling. As shown in Fig. 3(d),  $S(J)$  parameters exhibit the smooth variation which provides a good evidence for the chirality.

However, the newly assigned chiral-like pair bands in  $^{120}\text{I}$  have several differences from the known conditions needed to satisfy the chirality in the mass  $A \sim 130$  region. Firstly, the valence neutron in  $^{120}\text{I}$  is not a hole in character, but should be treated as a quasiparticle. In the mass  $A \sim 130$  region, the coupling of a proton particle and a neutron hole in the  $h_{11/2}$  orbital is one of optimal conditions, resulting in the occurrence of chiral pair bands. Secondly, the deformation in  $^{120}\text{I}$  exhibits a rather different aspect from the known chirality. One of the requirements is the aplanar angular momentum geometry caused by the triaxial deformation [7]. Consequently, the best condition is known to form the triaxial deformed potential with  $|\gamma| = 30^\circ$ . As shown in Fig. 3(e), however, the TRS calculations for the  $\pi h_{11/2}\nu h_{11/2}$  configuration in  $^{120}\text{I}$  indicate a  $\gamma$ -soft nucleus with a weak triaxial shape having  $\gamma \sim 13^\circ$ . This result is insufficient for satisfying the known chiral geometry in the mass  $A \sim 130$  region. In summary, the chiral-like pair bands in  $^{120}\text{I}$  satisfy neither the condition of a particle-hole configuration nor that of a triaxial deformation.

For studying the chirality built on the configuration of an  $h_{11/2}$  proton and an  $h_{11/2}$  neutron, Meng's group [23,24] investigated the angular momentum geometry in the framework of a particle rotor model with a quasi-proton and a quasi-neutron coupled with a triaxial rotor. After a detailed analysis, they found that the chiral geometry hold for away from the ideal case. The near-constant energy separation ( $\sim 200$  keV) between the partner bands was interpreted as being due to either a deviation of the core shape from  $\gamma = -30^\circ$  or a deviation of the Fermi energy surface from a particle-hole configuration. This is an outstanding feature that agrees with the case of  $^{120}\text{I}$  exhibiting a near-constant energy difference of 250 keV. However, our result still does not fully satisfy the theoretical predictions which require the  $\gamma$  condition as  $-40^\circ < \gamma < -20^\circ$ . Consequently, the observed doublet bands in  $^{120}\text{I}$  are supposed to be the chiral-like pair bands induced by the weak triaxial core with the  $\gamma$ -softness that shows the most striking difference. It is also worth noting that the observation of the doublet bands based on the  $\pi h_{11/2}\nu h_{11/2}$  configuration in  $^{120}\text{I}$  is the first case below  $Z = 55$ .

Now we turn our attention to an isomeric state. We notice that the  $16^+$  state at 5345 keV in  $^{120}\text{Te}$  is located close to the  $39/2^-$  state at 5186 keV in  $^{119}\text{Te}$  and the  $24^+$  state at 5410 keV relative to the  $10^+$  state in  $^{120}\text{I}$ . This  $16^+$  level in  $^{120}\text{Te}$ , being known to be an energetically favoured state, is a noncollective oblate shape built on the fully aligned four-quasiparticle  $\pi(g_{7/2}d_{5/2})_{6^+}^2\nu(h_{11/2})_{10^+}^2$  configuration. With this two-proton and two-neutron alignment in mind, we conclude that the  $24^+$  level can be formed by the  $\pi h_{11/2}\nu h_{11/2}$  orbital coupled to the  $16^+$  oblate structure, giving rise to an energetically favoured state with the  $\pi(g_{7/2})^1(d_{5/2})^1(h_{11/2})^1\nu(h_{11/2})^3$  configuration. Moreover, the 526-keV transition de-exciting the  $16^+$  level in  $^{120}\text{Te}$  is almost

**Table 1**

Summary of reduced transition ratios for Band 1 and Band 2. Intra-transitions and inter-transitions are notated as *in* and *out*, respectively. Uncertainties are given in parentheses.

Spin ( <i>J</i> )	$B(M1)_{in}/B(E2)_{in}$ ( $\mu_N^2/e^2b^2$ )	$B(M1)_{in}/B(M1)_{out}$	$B(M1)_{out}/B(E2)_{in}$ ( $\mu_N^2/e^2b^2$ )	$B(E2)_{in}/B(E2)_{out}$	$B(M1)_{in}/B(E2)_{out}$ ( $\mu_N^2/e^2b^2$ )
<b>Band 1</b>					
12	1.15(39)				
13	2.50(85)				
14	1.00(34)				
15	2.58(90)				
16	1.99(70)				
<b>Band 2</b>					
11		4.97(1.74)			
12	0.708(234)	1.77(60)	0.401(132)		
13	2.36(80)	97.9 <sup>a</sup>	0.024 <sup>b</sup>		
14	0.816(277)			36.6(13.2)	29.9(11.1)
15	2.59(83)			17.8(6.0)	46.2(18.0)

<sup>a</sup> Lower limit.

<sup>b</sup> Upper limit.

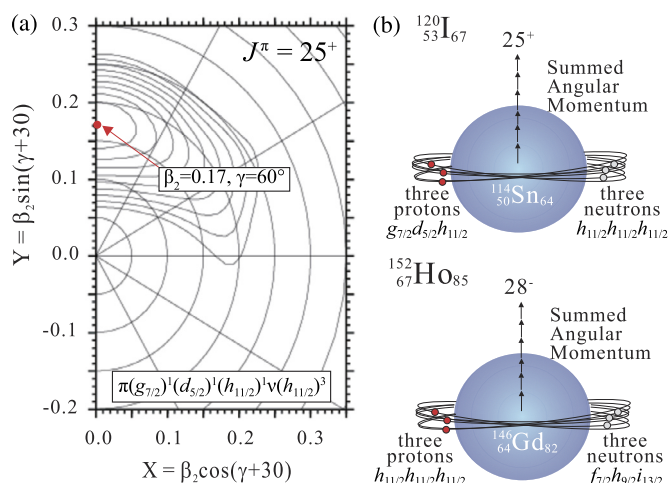


**Fig. 4.** (Colour online) (a) Plots of calculated total energy surfaces at  $J^\pi = 25^+$  by six quasiparticle alignments based on the  $\pi(g_{7/2})^1(d_{5/2})^1(h_{11/2})^1\nu(h_{11/2})^3$  configuration. (b) Schematic illustration of the high-angular-momentum isomers formed by aligning the six nucleonic orbitals for  $^{120}\text{I}$  and  $^{152}\text{Ho}$ .

identical to the 506-keV transition from  $24^+$  to  $22^+$  in  $^{120}\text{I}$ . Nevertheless, the contrast is apparent in two transitions. In  $^{120}\text{Te}$ , there is no evidence of an isomer with a half-life of a few or a few tens of nanoseconds but, in  $^{120}\text{I}$ , there appears an isomer with a half-life of few tens of nanoseconds. Therefore, the best explanation of the presence of the isomeric state is to assume the existence of a  $25^+$  level just above the  $24^+$  level at 6418 keV. This unusual high-spin state can be regarded as a noncollective oblate state and is responsible for the spin-trap isomer [25]. Our scenario is consistent with results of the TRS calculations, as shown in Fig. 4(a). Based on the TRS calculations, this isomer with the  $\pi(g_{7/2})^1(d_{5/2})^1(h_{11/2})^1\nu(h_{11/2})^3$  configuration, yielding  $J^\pi = 25^+$ , has a minimum energy at  $\beta_2 = 0.17$  and  $\gamma = 60^\circ$ . This result indicates that the  $25^+$  state forms a noncollective oblate shape with three quasi-protons and three quasi-neutrons. The SM calculations with the  $^{114}\text{Sn}$  core also support this scenario. According to the SM calculations, the absolute excitation energy of the calculated  $25^+$  state is located at 4.3 MeV. Although this value does not agree with the experimental result, it is important to notice that the relative energy gap between the calculated  $20^+$  and  $25^+$  states is consistent with the observed value, 1.4 MeV. Moreover, the calculated transitions from the  $25^+$  state are highly forbidden in terms of the reduced transition rates, which are  $0.02\mu_N^2$  and  $5.746e^2\text{fm}^4$  for the M1 and E2 transitions, respectively. This calculated  $25^+$  state is

dominated by the  $\pi(g_{7/2})^1(d_{5/2})^1(h_{11/2})^1\nu(h_{11/2})^3$  configuration, comprising 90%. Further, the calculations predict the oblate shape by providing the  $\beta_2$  parameter with the value of  $-0.1$ . This result is certainly consistent with the TRS calculations. Consequently, these two types of calculations strongly support that the isomer originated from the  $\pi(g_{7/2})^1(d_{5/2})^1(h_{11/2})^1\nu(h_{11/2})^3$  configuration with the noncollective oblate shape.

It is expected that an M1 transition, depopulating the  $25^+$  isomer, should be so low in energy that is giving rise totally to a conversion electron emission. If we assume that the M1 transition has an energy between 5 and 30 keV, then the corresponding reduced transition rate lies between 3.6 W.u. ( $6.46\mu_N^2$ ) and 0.016 W.u. ( $0.029\mu_N^2$ ). In  $^{152}\text{Ho}$  ( $Z = 67$ ,  $N = 85$ ), the isomer at  $28^-$  with a comparable half-life of 47 ns was found [26,27]. This isomer is known to be formed by six valence nucleon alignments,  $\pi(h_{11/2})^3\nu(f_{7/2})^1(h_{9/2})^1(i_{13/2})^1$ , outside the semi-double shell closure of  $^{146}\text{Gd}$  with  $Z = 64$  and  $N = 82$ . These two isomers have their own magic shells of 50 and 82, respectively, and share a semi-magic shell closure value of 64. Consequently, the  $25^+$  isomer is formed by six valence nucleon alignments,  $\pi(g_{7/2})^1(d_{5/2})^1(h_{11/2})^1\nu(h_{11/2})^3$ , having valence three protons and three neutrons outside the semi-double shell closure of  $^{114}\text{Sn}$  with  $Z = 50$  and  $N = 64$ . We demonstrate the present high-angular-momentum isomeric structure in Fig. 4(b), which schematically illustrates the summed high-angular-momentum  $25^+$  state formed by aligning individual valence nucleonic orbitals in  $^{120}\text{I}$  together with the  $28^-$  one in  $^{152}\text{Ho}$ . Finally, we propose the existence of an isomer at  $J^\pi = 26^-$  induced by the same physical phenomenon in  $^{138}\text{I}$ , in which three valence protons  $\pi(g_{7/2})^1(d_{5/2})^1(h_{11/2})^1$  and three valence neutrons  $\nu(h_{9/2})^1(f_{7/2})^1(i_{13/2})^1$  reside outside the doubly-magic nucleus  $^{132}\text{Sn}$  with  $Z = 50$  and  $N = 82$ .

In this work, we detailed the specific features observed in the excited levels of  $^{120}\text{I}$ : the chiral-like pair band for the  $\pi h_{11/2}\nu h_{11/2}$  configuration and the six-nucleon spin-aligned isomer at  $25^+$ . The positive-parity collective band built on the  $10^+$  level, and its partner band have been observed and are suggested to be associated with the chiral-like pair bands leading to a doubling of states for the  $\pi h_{11/2}\nu h_{11/2}$  configuration. This doublet structure is a unique feature in the  $Z = 53$  iodine nucleus and is regarded as the chiral band induced by a  $\gamma$ -soft weak triaxial core coupled with a proton and a neutron in the same  $h_{11/2}$  orbitals. Our observation of the first high-angular-momentum isomer at  $25^+$  indicates a spheroidal single-particle shell structure formed by aligning three protons and three neutrons outside the semi-double shell closure of  $^{114}\text{Sn}$  with  $Z = 50$  and  $N = 64$ . Our results provide a basic in-

gradient in understanding of proton–neutron interactions and the associated collectivity in nuclear many-body quantum systems.

### Acknowledgements

We would like to thank the technical staff of the ANU 14 UD accelerator for their support. Dr. C. Yuan acknowledges the National Natural Science Foundation of China (11775316).

### Appendix A. Supplementary material

Supplementary material related to this article can be found online at <https://doi.org/10.1016/j.physletb.2018.06.008>.

### References

- [1] P. Walker, G. Dracoulis, *Nature* 399 (1999) 35.
- [2] G.D. Dracoulis, *Phys. Scr. T* 88 (2000) 54.
- [3] P.M. Walker, G.D. Dracoulis, *Hyperfine Interact.* 135 (2001) 83.
- [4] S. Frauendorf, *Rev. Mod. Phys.* 73 (2001) 463.
- [5] V.I. Dimitrov, et al., *Phys. Rev. Lett.* 84 (2000) 5732.
- [6] S. Frauendorf, J. Meng, *Nucl. Phys. A* 617 (1997) 131.
- [7] K. Starosta, et al., *Phys. Rev. Lett.* 86 (2001) 971.
- [8] T. Koike, et al., *Phys. Rev. C* 67 (2003) 044319.
- [9] D.J. Hartley, et al., *Phys. Rev. C* 64 (2001) 031304(R).
- [10] R.A. Bark, et al., *Nucl. Phys. A* 691 (2001) 577.
- [11] S.P. Roberts, et al., *Phys. Rev. C* 67 (2003) 057301.
- [12] C.-B. Moon, et al., Annual Report, Department of Nuclear Physics, The Australian National University, 2002, pp. 11–12.
- [13] C.-B. Moon, et al., *J. Korean Phys. Soc.* 43 (2003) S100.
- [14] C.-B. Moon, et al., *J. Korean Phys. Soc.* 59 (2011) 1525s.
- [15] H. Kaur, et al., *Phys. Rev. C* 55 (1997) 512.
- [16] S. Törmänaen, et al., *Nucl. Phys. A* 613 (1997) 282.
- [17] Y. Liang, et al., *Phys. Rev. C* 45 (1992) 1041.
- [18] C.T. Papadopoulos, et al., *Z. Phys. A* 352 (1995) 243.
- [19] C.-B. Moon, et al., *Eur. Phys. J. A* 4 (1999) 107.
- [20] N. Shimizu, arXiv:1310.5431, 2013.
- [21] L. Li, et al., *Chin. Phys. Lett.* 30 (2013) 062301.
- [22] W. Nazarewicz, R. Wyss, A. Johnson, *Phys. Lett. B* 225 (1989) 208.
- [23] S.Y. Wang, et al., *Phys. Rev. C* 75 (2007) 024309.
- [24] S.Q. Zhang, et al., *Phys. Rev. C* 75 (2007) 044307.
- [25] Z. Szymanski, *Fast Nuclear Rotation*, Clarendon Press, Oxford, 1983, pp. 179–220.
- [26] S. André, et al., *Nucl. Phys. A* 575 (1994) 155.
- [27] M.A. Rizzutto, et al., *Phys. Rev. C* 55 (1997) 1130.
- [28] C.-B. Moon, et al., *J. Korean Phys. Soc.* 59 (2011) 1539.